6. Surface Engineering Artificial Heart Valves to Improve Quality of Life and Lifetime using Modified Diamond-like Coatings

6.1 Introduction

There are two types of artificial heart valves, namely, (i) biological valves and (ii) mechanical valves. Biological heart valves are made from tissue taken from animals or human cadavers. They are treated with preservatives and sterilized for human implantation. On the other hand, mechanical heart valves are made of man-made materials. The advantage of mechanical valves over biological valves is that they normally last for a comparatively longer lifetime. The biological valves exhibit a shorter lifetime and tend to wear out with time in service. This chapter discusses mechanical heart valves and highlights the underlying problems faced with biomaterials used in the manufacture of such valves. The history relating to mechanical heart valves will be reviewed, which dates back from 1952. We describe the principal cause of concern facing modern biomaterials used in the manufacture of heart valve components, which is thrombus formation (thrombosis). The hemocompatibility of biomaterials used in human implants will be discussed. Further, we describe the endothelium layer and discuss endothelial cell seeding as a tool for developing a heart valve that overcomes the common problems faced by modern valve materials. Diamond-like carbon (DLC) and its hemocompatibility and/or biological properties have been discussed and reviewed. Finally, we present results of endothelial cell seeding on chromium and silicon modified DLC films. A range of traditional and sophisticated techniques have been used to characterize the physical and biological properties of DLC and modified DLC films for applications in mechanical heart valves.

Heart disease is one of the most common causes of death in the world today, particularly in the western countries. There are various causes of heart disease, related most commonly to diet and exercise. The failure of heart valves accounts for about 25–30% of heart problems that occur today. Faulty heart valves need to be replaced by artificial ones using sophisticated and sometimes risky surgery. However, once a heart valve has been replaced with an artificial one there should be no need to replace it again and it should last at least as long as the life of the patient. Therefore, any technique that can increase the operating life of heart valves is highly desirable and valuable. Currently, pyrolytic-carbon (PyC) is used for the manufacture of mechanical heart valves. PyC belongs to the family of "turbostratic carbons", which have a similar structure to graphite.

Graphite consists of carbon atoms that are covalently bonded in hexagonal arrays. These arrays are stacked and held together by weak interlayer binding. PyC differs from graphite in that the layers are disordered, thus resulting in wrinkles or distortions within layers. This feature gives PyC improved durability compared to graphite. Although, PyC is widely used for heart valve purposes, it is not the ideal material. In its processed form, PyC is a ceramic-like material and like ceramics, it is subject to brittleness. Therefore, if a crack appears, the material, like glass, has very little resistance to the growth/propagation of the crack and may fail under loads. In addition, its blood compatibility is not ideal for prolonged clinical use. As a result, thrombosis often occurs in patients who must continue to take anti-coagulation drugs on a regular basis [1]. The anti-coagulation therapy can give rise to some serious side effects, such as birth defects. It is therefore extremely urgent that new materials, which have better surface characteristics, blood compatibility, improved wear properties, better availability and higher resistance towards breaking are developed.

6.2 History of Mechanical Heart Valves

Charles Hufnagel [2] was the first person, in 1952, to implant an artificial heart valve, in the form of Lucite tube and methacrylate ball, in the descending aorta of the heart with clamps that facilitated

rapid insertion of the valve without arresting the heart. Subsequently, the methacrylate ball was replaced with a hollow nylon ball coated with silicone rubber that was designed to reduce noise. More than 200 Hufnagel valves were implanted in patients with aortic insufficiency and remarkably some of these valves functioned for up to 30 years without any significant wear [3]. Later on Murray [4] employed a similar technique to insert a human homograph in the descending aorta.

Initially flexible polyurethanes and silicon rubber materials were employed for use in heart valve components. The reason for using such materials was that the valves would not only reside in the exact position anatomically but would effectively show mechanical characteristics similar to that of natural heart valves. Valves made from such materials were implanted in humans, in different ways. For example, in some cases, individual leaflet was made from flexible material and in others the entire valve was constructed from elastic materials. However, these elastic valves could not last longer than approx. 2–6 years due to a number of reasons, such as tearing, material fatigue and calcification [5-9].

In 1960, Dwight Harken [3,10] implanted double cage ball valves in seven patients. Unfortunately, only two of the seven patients survived the surgery. Later the same year, Albert Starr [3,10] was more fortunate than Dwight Harken, as he implanted prosthetic valve(s), comprising of metal cage and silicon ball, in a number of patients. The success rate increased as the number of survivals was six out of eight patients. These devices though proved durable but continued suffering from several problems like high profile, high rates of thromboembolism (blocking of blood vessel by a blood clot dislodged from its site of origin) and stenotic central position of the ball. Soon after in 1962, Vincent Gott and Ron Daggett [11] addressed two of the problems by introducing a low profile reinforced silicon flap valve that played a significant role in the reduction of central obstruction and the resulting valvular stenois in patients. In 1963, Antolio Cruz [12] devised a heart valve with a free-floating disc tilting on the edge of an orifice ring whose excursion was retained by a cage. Although it had good hemBODYnamic qualities, it was as stenotic as the ball valves and remained suffering from thromboembolic problems [10]. Wada-Cutter valve [13] was designed which significantly reduced

valvular stenosis and was thus first implanted in 1965. This valve enabled the disc to rotate or tilt about an axis slightly offset from the centre opening. With the Wada-Cutter valve, pivot points were fixed so that the stress and wear of the repeated openings was focused on two pivots on the disc. Later in 1974, its production was halted due to excessive wear of the Teflon occluder [10]. Subsequently, Don Shiley and Viking Bjork [3,10] designed a tilting disk valve known as the Bjork-Shiley valve. This provided the same features, as that of Wada-Cutter valves only with the difference that unlike it, the disk of the Bjork-Shiley valve was not fixed at pivots points [14]. In the original Starr-Edwards, Wada, Shiley prosthetic valves designs, instead of using the metal occluders, polymeric occluders were employed because of their lower density made for more light and more responsive moving parts. Owing to some key characteristics of plastics, plastic occluders were employed in heart valves. The elimination of strain flexure, considered essential for the elastic valves, increased the life of the more rigid plastic parts. But eventually all the polymeric occluders suffered from degenerative failure. Silicone balls would absorb lipids from the blood stream and crack if not cured appropriately [15]; Tefflon was subject to failure through cold flow from repeated stress in a focused location [16]; and Derlin would warp/distort in typical steam sterilization cycles as Derlin absorbs water and changes the configuration of the disc [3,17].

Gott [3,10] not just designed the first low profile heart valve but he contributed significantly in the field of biomaterials by performing a series of detailed investigations. Gott's experiments were performed on more than 200 dogs in which he implanted small tubes of different materials in vena cava in order to address thromboembolism through improvement in material selection [18]. The tubes made from polymer and stainless steel materials were used in the construction of heart valves in 1962 and it was found that they uniformly occlude within two hours. Later on it was discovered that an application of a coating made from graphite mixed with Heparin bonded with benzalkonium chloride removed clot formation in five animals for a period of up to two weeks. Lillehei and Nakib Ahmad [10] devised a non-tilting disk valve in 1967 that was entirely made of machined titanium, including the poppet and was called Lillehei-Nakib Toroidal Valve. A special division within a nuclear research company called

General Atomics was formed after Gott's publication on the biocompatibility of carbon and working here Dr Jack Bokros [3] developed a new carbon material called Pyrolite (also known as pyrolytic carbon). Eventually, in 1969, after more than six years of development, plastic and metal materials used for heart valves started to become replaced by Pyrolite. Michael DeBakey [19] implanted a valve that was very similar to Starr aortic valve with a hollow pyrolite ball as occluder. Taking advantage of the improved biocompatibility and durability of pyrolytic carbon, translating disk valves like the Beall-Suritool and Cooley Cutter valve were redesigned [120]. Later in 1974, Shiley valve became the most frequently implanted mechanical valve just after when the Derlin disk in the Shiley valve was changed to pyrolytic carbon [21].

The Lillehei-Kaster (LK) [22-23] tilting disk was introduced in 1970 with a pyrolytic carbon disk and solid titanium orifice and it has a remarkable record of 30 years with only one case reported of structural failure. In 1976, the valve was redesigned by replacing flat disk by a curved disk, which in turn, improved the catastrophic thrombosis [3,21,24]. Further improvement was achieved later in 1984 when the orifice was changed from titanium to Pyrolite carbon [3, 25].

Bob Kaster [26] redesigned the LK valve that was introduced seven years ago, by replacing the outflow struts with a single wire running through the centre of the disk. Although the efficiency of this valve was reduced due to the hole through the centre of the disk allowing increased blood leakage through it yet this device maintained the excellent reliability of the original LK design. The only reported structural failure for this design was combated by changing the flat disk to a rounded surface in a D-16 design in order to avoid the observed impacts of disk with the large flat stop when it closes [27]. Basically this change was implemented in order to reduce haemolysis but this change resulted in three reported cases of disk fracture when combined with Pyrolite disk attached to the extremes of the allowable tolerances.

Today, heart valves employing two leaflets in their design are implanted but the idea of bileaflet valve was documented by John W. Holter in 1958 the time when valves were still being implanted in the descending aorta. In 1963, Vincent Gott and Dr. Ronald Daggett

developed a valve called “Gott-Daggett valve”, which was a polycarbonate ring containing a disc of Teflon fabric impregnated with silicone rubber [28]. Then Dr Lillehei implanted an all titanium bileaflet valve in 1968 that was developed by Kalke [29] but the patient died within 48 hour so the idea was abandoned. After seven years, the founder of cardiac pacemakers designed a valve very similar to the Kalk Valve (with little modifications) and requested Carbomedics to build it from Pyrolite carbon. This design known as “St Jude Medical heart valve” was the first that was entirely made up of pyrolytic carbon [10, 21] and quickly captured a leading market position. Although this valve had design and material improvement as major factors in its growth but its market acceptence was also pushed up due to strut failure problems in the Shiley valve [30].

The combination of Pyrolyte carbon with a bileaflet valve proved significant but it failed to provide a cure for the patients with prosthetic valves. Soon after five years of the introduction of St Jude’s valve, a new valve Baxter-Duromedics [31] entered the market with an improvement in pivot design and with a seating lip that the occluders rest against in the closed position. The seating lip proved effective in reducing the regurgitation but the desired gain in the efficiency was counterbalanced by the loss of orifice area. Further the seating lip enhanced the formation of cavitation bubbles that resulted in significant structural damage and thereby the design was withdrawn after 3 years with only 20,000 valves due to 12 reported cases of structural failure [32].

Sulzer Carbomedics [33] introduced a new bileaflet valve called the Carbomedics Prosthetic Heart Valve (CPHV) in 1986, which improved the pivot design with a titanium stiffening ring to protect the valve. The implant of over 325,000 of these valves in 14 years with no post-operative structural failure demonstrated clearly the effectiveness of titanium stiffening ring. Sorin Biomedics [34] who had been manufacturing tilting disc valves similar to Shiley valves started offering a bileaflet valve as well in 1990. Sorin combined a curved pyrolitic carbon leaflet, similar to Baxter Duromedics design with a titanium orifice. The titanium orifice was basically used both to avoid expense and manufacturing complexities associated with Pyrolitic carbon. The Sorin valve was coated with a thin layer of vapour deposited carbon on the titanium. Later Edward Life Sciences

[35] obtained the rights of marketing this valve in U.S with little modification in the new sewing ring design with oversized silicon filler but otherwise left the design unchanged. Several independent investigators came up with the conclusion that the carbon layer is subjected to rapid erosion both in vivo and in vitro explaining the limited acceptance of the Sorin bileaflet and Edwards Mira valve [35]. Sorin [36-37] accepted the need for further studies after knowing that insufficient safety and effectiveness data had been collected for this valve.

In cooperation with the Carbon implants, the Medtronic [21] company began a clinical study and designed Medtronic Parallel Valve to open parallel to the flow of blood with a 90° opening angle rather than the 78-80° angles used by other manufactures. Pivot in this valve was quite complex, intended to decrease the leakage when the valve was fully closed, and it has been shown to be an important risk factor for valvular thrombosis [38]. Hence it was withdrawn from the market within one year of clinical trials.

Certain employees of Carbon Implants, Inc. formed a spin-out company called as Medical Carbon Research Institute (MCRI) after completing the design of the Medtronic Parallel Valve and developed another valve similar to this. This new valve was called the On-X™ [21] with an elongated orifice, 90° opening angle and 40° closed angle featuring four sizes of carbon orifices labelled 19, 21, 23, and 25 mm. Finally in 1999, Medtronic began another bileaflet valve clinical trail in Europe with an internally developed bileaflet valve called the Medtronic Advantage [34].

Two of the most recent valves are the ATS Open Pivot® bileaflet valve and the On-X® prosthetic valve [39]. ATS open pivot valve (made by ATS Medical, Inc. in 2000) is a mechanical heart valve with two leaflets (flap like structures) in the shape of a circle, each leaflet is half the circle, surrounded by a ring made of polyester fabric. The leaflets are made of carbon.

The On-X® valve (made by Medical Carbon Research Institute, LC in 2001) is a mechanical heart valve with two movable half-discs (bileaflets), contained within a housing surrounded by a man-made fabric-covered ring. The leaflets are made of graphite and tungsten, with a carbon coating.

Table 6.1. Summary of the material composition of nine key designs of mechanical valves developed since 1959

Year	Valve Name	Type	Poppet	Material
1959	Hfnagel	Ball	Polypropylene	Methacrylate
1964	Starr-Edwards 1000	Ball	Silastic	Stellite
1968	Wada-Cutter	Tilting Disc	Teflon	Titanium
1969	Bjork-Shiley	Tilting Disc	Derlin	Stellite
1970	Lillehei-Kaster	Tilting Disc	Pyrolitic carbon	Titanium
1971	Bjork-shiley	Tilting Disc	Pyrolitic carbon	Stellite
1977	Medtronic-Hall	Tilting Disc	Pyrolitic carbon	Titanium
1977	St Jude Medical	Bi-leaflet	Pyrolitic carbon	Pyrolitic C
1991	Jyros	Bi-leaflet	Vitreous carbon	Vitreous C
1999	Medtronic Advantage	Bi-leaflet	Pyrolitic carbon	Pyrolitic C

Mechanical heart valves can be classified into three primary types: (i) ball and cage, (ii) tilting disk, and (iii) bileaflet valves. Table 6.1 shows the types of heart valves used for implantation since 1959. All mechanical heart valves consist of an occluder working as an element to retard the flow of blood and of a mechanism to restrain the motion of the occluder. The occluder functions relatively in response to the pressure across the valve during the cardiac cycle. The occluder opens to permit the blood flow through the valve in case if the upstream pressure is greater than the downstream pressure and closes when the downstream pressure is greater than the upstream pressure to stop the blood flow through the valve. Figure 6.1 shows a typical mechanical heart valve made by Medtronic, USA.

Fig. 6.1. A typical PyC leaflet heart valve (Medtronic)

6.3 Thrombosis

As mentioned earlier, the principal concern with mechanical heart valves is thrombus formation. The process of a blood clot (thrombus) formation inside a blood vessel to stop bleeding is termed as thrombosis. Excessive blood loss is undesirable and physiological feedback systems exist for protection. Therefore, the body has ways of protecting itself in cases when the blood escapes the body. When the human body loses a small amount of blood through a minor wound, the platelets cause the blood to clot in order to stop the bleeding. Because new blood is always being made by hemopoetic stem cells located in bone marrow, the body can replace the lost blood effectively and efficiently. However, when the human body loses a large amount of blood through a major wound, then in such cases blood needs to be replaced through a blood transfusion from other people.

Clotting involves thrombus formation that prevents further blood loss from damaged tissues, blood vessels or organs. Figure 6.2 shows the schematic of the thrombosis process. The first step in the clotting process is the adsorption of blood proteins on the skin surface. There are three types of proteins in human blood: (i) albumin, (ii) fibrinogen and (iii) globulin. Albumin, fibrinogen and globulin are present in the blood in the following percentage (%) ratio: 60:4:35, respectively. Soon after vessel injury occurs, blood clotting is initiated resulting in platelets and tissues to secrete a clotting factor called prothrombin activator. Prothrombin activator and calcium ions catalyse the conversion of prothrombin to thrombin (activated form), which subsequently catalyses the conversion of fibrinogen to fibrin threads. Fibrin threads are sticky and trap more platelets thus further sealing the point of blood leak.

Platelets are irregularly shaped, colourless bodies that are present in the blood. Their sticky surface enables them, along with other substances, form clots at the blood outlet point(s) to stop bleeding. The mineral calcium, vitamin K and fibrinogen help the platelets form a clot. If blood is lacking these nutrients, it will take longer than normal for the blood to clot. If these nutrients are missing, one could bleed to death. Some clots can be extremely dangerous. A blood clot that forms inside of a blood vessel can be deadly because it blocks the flow of blood, cutting off the supply of oxygen to the body.

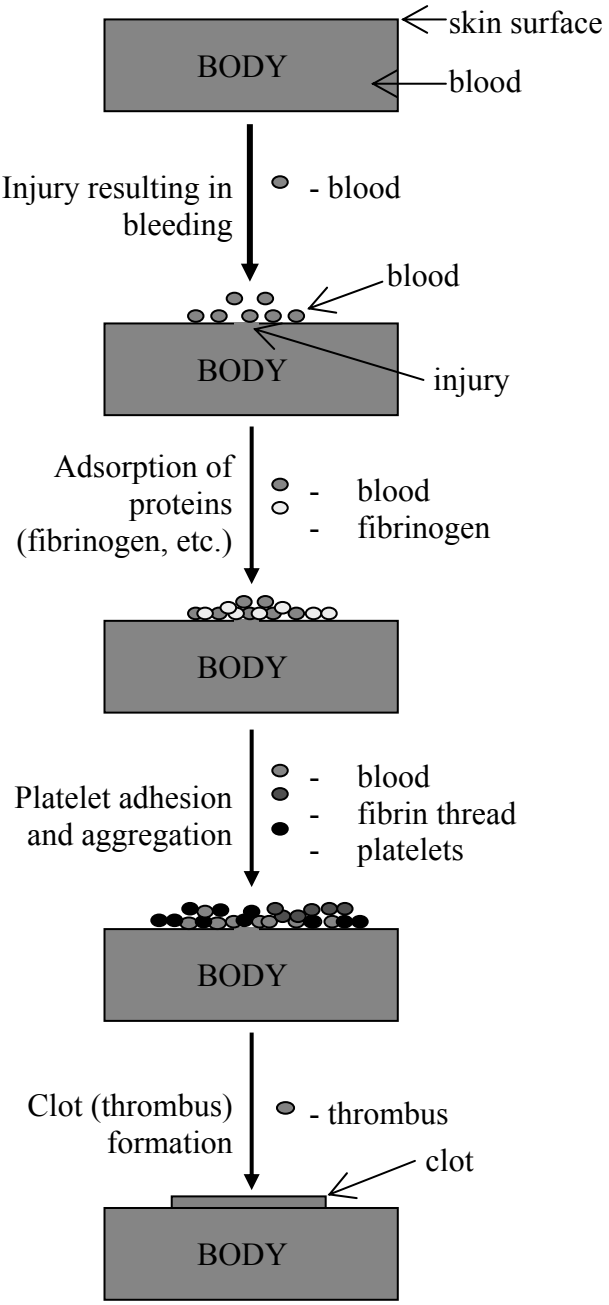

Fig. 6.2. Schematic diagram depicting the thrombosis process in the human body

There are two pathways that effectively lead to the formation of a blood clot, namely, the intrinsic and extrinsic pathways. Although they are initiated by distinct mechanisms, the two converge on a common pathway that leads to clot formation. The formation of a blood clot in response to an abnormal vessel wall in the absence of tissue injury is the result of the intrinsic pathway. Thrombus formation in response to tissue injury is the result of the extrinsic pathway. Both pathways are complex and involve numerous different proteins termed clotting factors.

There are many circumstances that may lead to thrombosis, however, the principal three situations include: (i) damage to endothelial cells, which line the interior surface of blood vessels; (ii) slow blood flow; and (iii) changes in the composition of blood. There are many ways endothelial cells can be damaged. For example, increased blood pressure (hypertension) is one common cause of endothelial damage. Diseases of blood vessel walls [40] (e.g., atherosclerosis) can damage endothelial cells directly or roughen the endothelial lining producing turbulent blood flow that, in turn, damages endothelial cells. If blood flow becomes abnormally slow, platelets have the opportunity to contact the endothelial lining. Once the platelets are in contact they may stick and initiate the intrinsic blood coagulation pathway. Similarly, other conditions may indirectly initiate blood clotting. For example, certain alterations in red blood cells (e.g., some anemias) can make them stickier than normal resulting in clumping of RBCs (erythrocytes) and reduced blood flow. Similarly, overproduction of RBCs (polycythemia) can cause the blood flow to slow.

6.4 Hemocompatibility

Hemocompatibility can be defined as the implanted material's compatibility with the blood. This definition takes into account the following [41]:

- The activation of the blood coagulation system at the blood-material interface
- The response of the immune system induced after the blood-material contact
- The other tissue responses which appear as consequence of the blood-material contact

The hemocompatibility of the implant material is closely related to the reactions between the surface of the biomaterial and the inflammatory host response [42]. There are several factors that contribute to this and these may depend on individual patient characteristics, such as general health, age, tissue perfusion, immunological factors, or implant characteristics, such as surface roughness and porosity, chemical reactions at the surface, corrosion properties of the material, and the toxicity of the individual metals present in the alloy [43].

The human body is able to resist against any form of attack from unknown foreign material(s). When a material (foreign body) is implanted in the human body, it comes in direct contact with blood. This contact between the blood and material leads to an inflammatory reaction directed against the material. The following are some of the interactions that can be considered either as good or bad depending on the circumstances [44]:

1. Adsorption of proteins, lipids, or calcium from the blood onto the surface of the device. At a later step, migration of the surface adsorbed material into the bulk may occur.
2. Adhesion of platelets, Leukocytes or erythrocytes onto the surface of the device.
3. Formation of "capsules" on the outer surface of the device, or "pseudo-intima" on the inner surface of a device, e.g., for a vascular graft.

The interactions that are generally regarded as undesirable are as follows [45]:

1. Platelet activation and aggregation.
2. Formation of thrombi (blood clot) on the device surface.
3. Transport of thrombotic or other material from the surface of the device to another site via the circulatory system.
4. Injury to cells or tissues adjacent to the device.
5. Injury to circulating blood cells, e.g., Hemolysis (Hemolysis is the breakage of the red blood cell's (RBC's) membrane, causing the release of the hemoglobin and other internal components into the surrounding fluid).

6. Overenthusiastic cell proliferation (increase in cell number by division) on or adjacent to the device resulting in reduced or turbulent blood flow of the blood at the device location.
7. Adsorption of proteins, lipids, or calcium from the blood onto the surface of the device.

The surface of the biomedical device implanted in the body is critically important because it comes into direct contact with the surroundings (i.e., tissues, blood, etc). It is the response of the host to the material that defines the character of the biomaterial that is used in medical surgery. Surface roughness/smoothness is another important parameter, which can have a noticeable influence on the hemocompatibility of a biomaterial carrying the surface. For example in artificial heart valve applications, a smooth surface is essential as surface roughness causes turbulence in the blood, which leads to the integrity of the red cells being damaged causing bacteria to adhere, and blood coagulation and clots.

A relationship has been proposed between surface charges on materials and protein deposition levels on such surfaces [46]. It has also been stated that the biocompatibility of materials can be influenced by factors such as hydrophobicity and topography [47, 48]. Reports from Ahluwalia et al. [49] and Bowlin and Rittger [50] based on surface potential measurements using the vibrating Kelvin probe method suggest that positively charged surfaces enhance cell adhesion in comparison to neutral or negatively charged surfaces. The hydrophylic or hydrophobic nature of a surface has also been associated with the extent of cell interactions with the surface [49,51]. There has also been suggestions in the literature that the electron conduction of materials might have an effect on their biocompatibility. Bruck [52, 53, 54] reported, based on his studies on pyrolytic polymers, that intrinsic electronic conduction and semi-conduction may be involved in the extent of hemocompatibility observed in the materials. Bruck [52, 53, 54] observed clotting times, six to nine times longer than those observed with non-conducting polymers and also observed little or no platelet aggregation in electro-conducting polymers, when compared to non-conducting control samples.

Boldz and Schaldach [55] and Chen et al. [56] have also reported that there is a relationship between the electronic structure of a

surface and it's hemocompatibility. According to these authors [55, 56], the denaturing of fibrinogen at a surface involves an electron transfer from the inactive site of the protein to the surface of the solid, i.e., an oxidation process takes place (a redox reaction). They suggested that fibrinogen decomposes after the electron transfer and transforms into fibrin-monomer and fibrin-peptides, with a cross-linking to form thrombus. Fibrinogen has been reported to have an electronic structure similar to a semiconductor [55] and a band-gap of ~1.8ev. Boldz and Schaldach [55] have suggested that haemocompatible surfaces will be expected to have a low density of unoccupied states in the energy range of the transfer level with an energy band-gap of greater than 1.8eV. Their reasoning was that if the charge transfer energy range lies in the band-gap energy range of the artificial surface, the oxidation process involving electron transfer is inhibited. It is well known from the theory of hetero-junctions, that when the band-gap of a semiconductor is contained within the band-gap of another semiconductor (i.e., straddling hetero-junction), electrons and holes need energy (ΔEc and ΔEV) respectively to move from the semi-conductor with the small band-gap to the one with the larger band-gap. ΔEc and ΔEV represent the differences of the conduction and valence band edges of the two semiconductors.

6.5 Endothelium and Endothelial Cell Seeding

Endothelium is the layer of thin, flat cells that line the interior surface of blood vessels, forming an interface between circulating blood inside the vessel and rest of the vessel wall. All blood vessels and lymph vessels (a network of vessels throughout the body that drains fluid from tissues and returns it to the bloodstream, managing fluid levels in the body, filtering out bacteria, and housing types of white blood cells.) are lined with endothelial cells; the layer being called the *endothelium.*

Under normal circumstances the endothelial surface prevents blood clotting and allows smooth flowing of the blood thus controlling blood pressure [57]. Surface molecules of endothelial cells act as receptors and interaction sites for a whole host of important molecules, especially those that attract or repel WBCs (leucocytes*).* Leucocyte

adhesion molecules are important in inflammation and are normally repelled by endothelium in order to allow the free flow of blood cells over the surface. But in inflammatory states the WBCs are actually attracted to the endothelium by adhesion molecules. In addition platelets start sticking to the surface and later to each other making a network that end up making a clot [58].

Endothelium is known as "nature's haemocompatible surface", and the performance of any biomaterial's hemocompatibility must be compared with that of the endothelium [59].

A promising and logical approach to reduce thrombogencity is endothelial cell seeding to synthetic vascular grafts. Endothelial cell function on synthetic grafts can be improved by inserting genes to reduce or inhibit thrombus formation. The graft can be modified to release agents, which inhibit smooth muscle cell growth and promote endothelial cell adhesion and function. For synthetic grafts with diameters less than 6 mm, vascular graft acceptance requires an endothelial monolayer on the graft's luminal surface to reduce thrombosis. Grafts are seeded with endothelial cells prior to insertion in the body in order to encourage the development of a monolayer of endothelial cells. Seeding and implantation must occur rapidly in order to minimize the chance of infection [60]. Otherwise, a confluent endothelial monolayer will not form and a subconfluent layer of endothelium will be exposed to fluid shear stresses, resulting in complications. Endothelial cell adhesion to a synthetic surface involves a defined set of molecular interactions that influence subsequent cell division and/or protein synthesis. Endothelial cell adhesion to vascular grafts involves:

1. attachment and spreading on a rough synthetic surface;
2. maintenance of attachment following exposure to blood flow;
3. normal function.

Experimentally, cell adhesion to foreign biomaterials, such as polymers is influenced by manipulation of the following variables:

1. The surface properties which influence non-specific and specific interactions (e.g., hydrophobicity, surface charge, presence of oxygen and amine groups);

2. The density and affinity of adhesion molecules on the surface;
3. Covalent and non-covalent interactions between the cell and surface molecules;
4. The time of interaction between the cell and the surface;
5. Signalling events within the cell to promote or inhibit cell spreading.

Cell attachment and spreading on artificial surfaces is mediated by bonds formed between cell adhesion proteins at the substrate surface and protein receptors embedded in the cell membrane. The role of adsorbed proteins in cell adhesion has been reviewed elsewhere [61].

6.6 Surface Engineering Artificial Heart Valves

In the following section(s) we focus on biocompatible coatings used to improve the surface characteristics of blood contacting devices, such as mechanical heart valves in order to overcome thrombus formation.

6.6.1 Biological Properties of Diamond-like Carbon

Diamond like carbon (DLC) is a very promising coating because it is chemically inert, extremely hard, wear resistant and biocompatible [62, 63]. Biological properties of DLC can be altered by alloying [64, 65, 66, 67]. DLC, as a biocompatible base material, can be easily alloyed with other biocompatible materials such as titanium or silicon, or toxic materials such as silver, copper and vanadium [68].

In the investigation of hydrogen free DLC, test results show that the higher bonding ratio of sp^3/sp^2 may contribute to the blood compatibility of DLC. However, as the DLC films doped with nitrogen of certain concentration, even if the bonding ratio of sp^3/sp^2 is decreased, the behavior of platelet adhesion can be improved significantly [69]. A similar phenomenon has been observed in hydrogen free DLC film doped with argon [70]. As argon atoms are introduced into DLC to a certain content, the bonding ratio sp^3/sp^2 of the DLC films changes from 78/22 to 56/44, and the platelets adhesion behavior of the films is modified significantly. It is also found that above phenomena may be related to changes in surface tension on the

films. If DLC films are annealed at the temperature of 600℃, the DLC films present a p-type characteristic. The blood compatibility becomes deteriorated [71,72]. The DLC film, which has a more hydrophilic nature, seems to have better blood compatibility than that of the DLC film with more hydrophobic nature [73].

The platelet adhesion is reduced on DLC when compared with Ti surface. Jones et al. [74,75] showed by In vitro experiments that the DLC surfaces expressed a decreased area coverage of platelets compared to titanium, TiN and TiC. Whereas on the Ti containing surface platelet activation, clotting of platelets and thrombus formation was observed, no such reaction took place on the DLC surface. High albumin to fibrinogen ratio was also observed in DLC as compare to Ti, TiN and Tic coatings which is an indication of the ability of DLC to prevent thrombus formation [75]. Dion et al. [76] also observed higher albumin/fibrinogen ratio in DLC as compare to silicone (a polymer widely used for implants). Cui and Li [77] state from in vitro experiment that DLC and CN films show good tissue- and blood compatibility.

Gutebsohn et al. [78] analysed the intensity of the platelet activation antigens CD62p and CD63 and showed that DLC coating of a stainless steel coronary artery stent resulted in a decrease of these antigens. It indicates a low platelet activation on DLC and, therefore, a low tendency for thrombus formation. In this in vitro experiment, they showed that DLC coating suppressed metal ion release from the stainless steel stent which may influence negatively the hemocompatibility of the surface. Alanazi et al. [79] conducted an in vitro experiment using a flow chamber and whole human blood, which showed a low percentage of DLC to adhere to the surface. However, the results differed with the deposition conditions used to produce DLC:

Thomson et al. [80] have studied the inflammatory potential of DLC-coated tissue culture plates by measuring the levels of the lysosomal enzymes released from macrophages cells (cells play major role in inflammation and the response to foreign bodies). They showed that no inflammatory response was elicited in vitro. Similarly Fibroblast is another cell used to test biocompatibility. Preliminary result [81] showed no statistically significant differences between fibroblasts grown on in control polystyrene plate and those grown in DLC coating.

Some work has been done showing change in bioreaction on DLC due to alloying [82, 83, 84, 85, 86, 87, 88]. A reduced inflammatory reaction was observed on implanted stents when SiO_x was added to DLC [82]. It was noticed that proteins adsorption could be altered as a function of Ti content [85, 87] in the DLC Osteoclasts (osteoclast is a large multinucleated cell that plays an active role in bone resorption) was inhibited by the addition of Ti into DLC [83, 84]. The addition of Ca-O to a DLC film resulted in decreased wetting angle, improved cell morphology and viability of mouse fibroblast cells [88].

6.6.2 Other Biocompatible Coatings

It is worth considering that titanium and its alloys have been used in biomedical implants for many years now and therefore it is sensible to look at the surface treatment of titanium alloys for producing superior surface characteristics, which could be ideal for heart valves. It should be noted that titanium alloys are not brittle like PyC. A large number of research scientists have deposited Ti-based coatings, using energised vapour-assisted deposition methods, and studied their potentials for use in biomedical areas, such as heart valves or stents. Yang et al. [89] deposited Ti-O thin films using plasma immersion ion implantation technique and characterised the anti-coagulant property employing in-vivo methods. They found that the Ti-O film coatings exhibited better thrombo-resistant properties than low-temperature isotropic carbon (LTIC), in long-term implantation. Chen et al. [90] deposited TiO coatings doped with Ta, using magnetron sputtering and thermal oxidation procedures, and studied the antithrombogenic and hemocompatibility of $Ti(Ta^{+5})O_2$ thin films. The blood compatibility was measured in-vitro using blood clotting and platelet adhesion measurements. The films were found to exhibit attractive blood compatibility exceeding that of LTIC. Leng et al. [91] investigated the biomedical properties of tantalum nitride (TaN) thin films. They demonstrated that the blood compatibility of TaN films was superior to other common biocompatible coatings, such as TiN, Ta and LTIC. Potential heart valve duplex coatings, consisting of layers of Ti-O and Ti-N, have been deposited onto biomedical Ti-alloy by Leng et al. [92] and their blood compatibility and mechanical properties have been characterised. The TiO layer was designed to improve the blood

compatibility, whereas, TiN was deposited to improve the mechanical properties of the TiO/TiN duplex coatings. They found that the duplex coatings displayed (i) better blood compatibility than LTIC; (ii) greater microhardness; and (iii) improved wear resistant than Ti6Al4V alloys. It has been reported that the TiO coatings display superior blood compatibility to LTIC [93].

6.6.3 Chromium Modified DLC

Chromium modified DLC (Cr-DLC) films with varying %Cr content were deposited on 50 mm circular silicon wafers using magnetron sputtering utilising the intensified plasma assisted processing (IPAP) process [94]. Table 6.2 shows the conditions employed to deposit the Cr-DLC samples with varying %Cr contents. The as-deposited Cr-DLC films were nanocomposite and consisted of nano-sized chromium carbide particles embedded in an amorphous DLC matrix.

Figure 6.3 shows the XRD spectrum for a typical Cr-DLC film, with 10%Cr, in the 2-theta range 15-115 degrees. It was found from HRTEM studies that the nano-structured Cr-DLC film consisted of nano-sized (5 nm) chromium carbide particles. The presence of chromium carbide particles was evident from the XRD peak centered at around 33°2-theta value. The other major intense peak centered at around 68°2-theta value corresponds to silicon, which was from the silicon wafer substrate material. We found that the Cr-carbide nanoparticles were embedded deep into the amorphous DLC matrix and were not present on the DLC surface. This enabled the nano-particles to be protected by the amorphous DLC film.

Table 6.2. Deposition parameters employed in depositing Cr-DLC films using the IPAP process

Sample	Deposition rate (nm/min)	Magnetron Current (mA)
Cr(1%)DLC	6.6	155
Cr(5%)DLC	7.6	220
Cr(10%)DLC	15.2	310

Bias Voltage: -1000 V; flow rate (sccm): CH_4:Ar 7.4:40;
Chamber pressure: 2.66 Pa; processing time: 2 hrs;
sputter cleaning: Ar^+: 3.3 Pa, -1500 V, ~20 minutes.

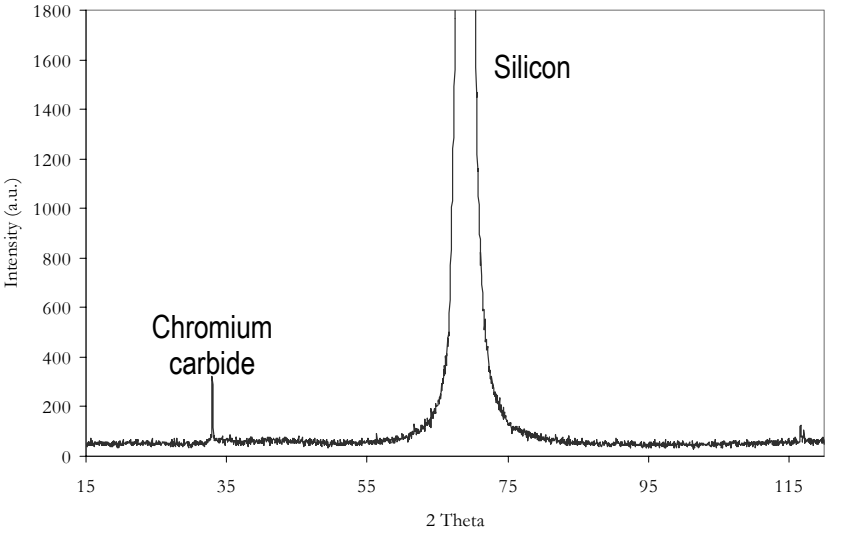

Fig. 6.3. XRD spectrum for sample Cr(10%)-DLC showing the silicon substrate and chromium carbide peaks

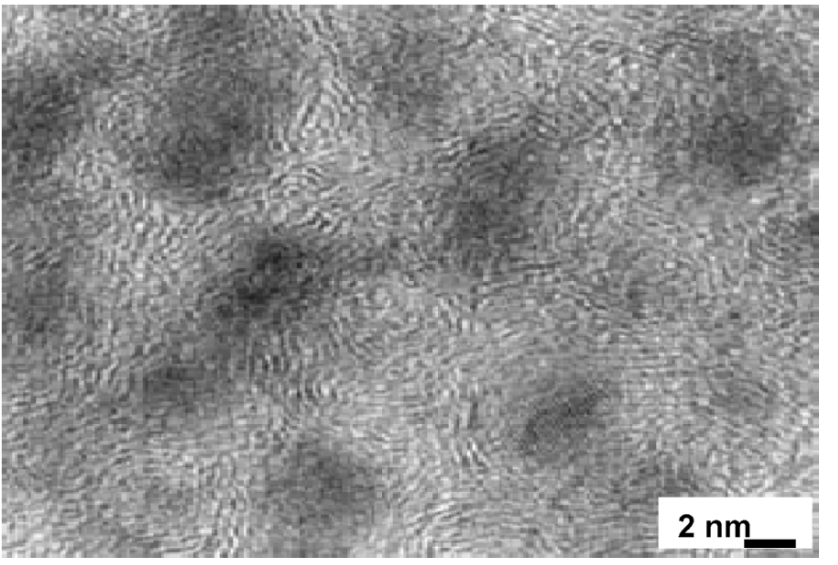

Fig. 6.4. High Resolution TEM micrograph of the 5%Cr-DLC sample showing the microstructure exhibited by the thin film coating

Figure 6.4 Displays the high-resolution (HRTEM) micrograph representing 5%Cr-DLC and showing the microstructure exhibited by the same as-deposited film. The micrograph shows the presence

of nanoclusters (NCs) around 5 nm in diameter surrounded by a ~2 nm thick amorphous matrix. Electron diffraction showed that the dark contrast NCs correspond to Cr carbide, encapsulated by an amorphous matrix.

The contact angle measurements obtained using the optical method are as shown in Figure 6.5. Chromium doping leads to a gradual increase in the contact angles as shown in Figure 6.5. The increase begins to level out with Cr content above 5% where it begins to reach saturation point. The average contact angles displayed by samples 1%Cr-, 5%Cr- and 10%Cr- DLC samples were calculated to be 80.285, 97.23 and 99.274 degrees, respectively. Raman spectroscopy was used to characterise the quality of the as-deposited Cr-DLC films with different Cr contents, in terms of diamond carbon-phase purity. The data from the Raman spectroscopy studies, including intensities of D (I_D) and G (I_G) bands, Full width at half maximum (FWHM) of I_D and I_G bands, I_D/I_G ratio and the positioning of the D and G band peaks can all be found in Table 6.3. From the Raman investigations, it was found that the Cr-DLC films displayed the two D and G bands of graphite. The G and D bands are usually assigned to zone centre of phonons of E_{2g} symmetry and K-point phonons of A_{1g} symmetry, respectively. The D band peaks for the three Cr-DLC films were positioned at 1401.6, 1408.4 and 1306.8 cm^{-1}, whereas, the G band peaks were centered at 1538.8, 1540.6 and 1511.8 cm^{-1}. From both D and G bands, 5%Cr-DLC sample displayed the smallest values for FWHM. The I_D/I_G ratio was the least for 10%Cr-DLC and the highest out of the three samples for the 5%Cr-DLC film. This suggests that there are more disordered graphitic phases in sample 5%Cr-DLC and the least similar disorder in 10%Cr-DLC film.

The results of the cell count analysis shown in Figure 6.6, give an indication of the influence of Cr content in Cr-DLC films on the adherent cell population of the three samples, 5%Cr-DLC provided the best conditions for HMV-EC seeding, while, 10%Cr-DLC film resulted in the least population of adherent human endothelial cells onto its surface. It should be noted that sample 1%Cr-DLC was a better base material for seeding endothelial cells than 10%Cr-DLC. Figure 6.7 displays the SEM micrographs showing the population of endothelial cell attachment onto 1%Cr-, 5%Cr- and 10%Cr- DLC film surfaces. All three films displayed smooth surface profiles, which is a key requirement in artificial heart valve applications.

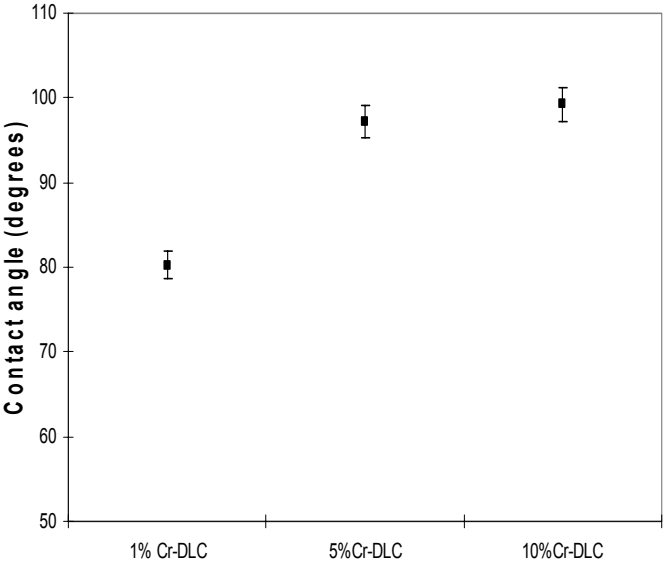

Fig. 6.5. Graph showing the contact angle measurements as obtained using the optical method for the three Cr-DLC samples

Table 6.3. Raman data obtained for the three Cr-DLC samples. The data includes I_D and I_G peak intensities; Full-Width at Half Maximum (FWHM) values for D band; and D and G band intensities

Sample	%Cr	I_D (a.u.)	I_G (a.u.)	FWHM (D)	D-Peak (cm^{-1})	G-Peak (cm^{-1})
CrDLC1	1	21.833	21.043	363.68	1401.6	1538.8
CrDLC2	5	21.628	20.415	361.08	1408.4	1540.6
CrDLC3	10	45.588	49.748	389.90	1306.8	1511.8

It was noted that there was a direct correlation between the I_D/I_G ratio and the population of endothelial cells attaching to the three Cr-DLC films with different Cr contents. We noted that from the three Cr-DLC films, the highest value displayed for the I_D/I_G ratio was by 5%Cr-DLC film, which also gave the highest adherent cell population onto its surface. The lowest I_D/I_G ratio value was for 10%Cr-DLC, which showed the least, from the three samples investigated in this study, population of cell attachment to its surface after conducting the cell seeding procedures. Furthermore, the density of nano-sized

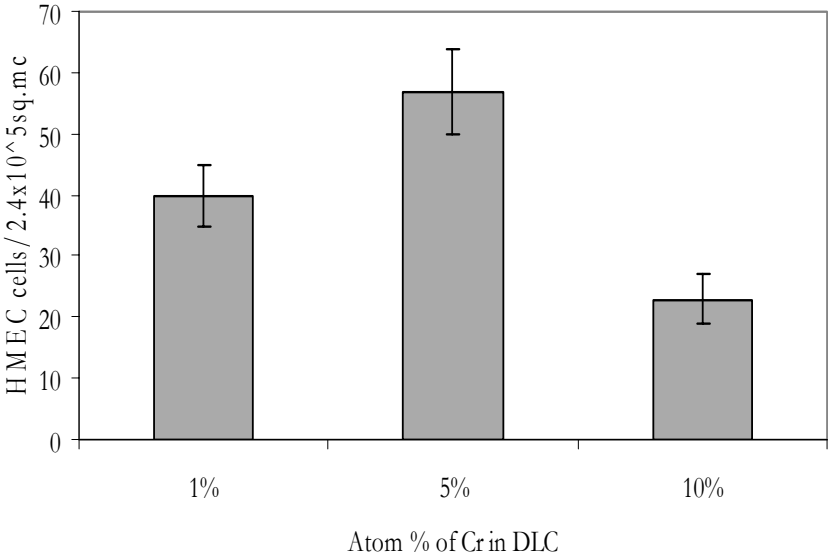

Fig. 6.6. Graph showing the cell count results obtained after seeding the human microvascular endothelial cells onto the Cr-DLC surfaces

Cr-carbide particles produced during film growth is expected to be the highest in 10%Cr-DLC and the least in 1%Cr-DLC sample. This difference in the Cr-carbide content in the three films is sure to influence the surface chemistry of the DLC films.

It was noted that there was a direct correlation between the I_D/I_G ratio and the population of endothelial cells attaching to the three Cr-DLC films with different Cr contents. We noted that from the three Cr-DLC films, the highest value displayed for the I_D/I_G ratio was by 5%Cr-DLC film, which also gave the highest adherent cell population onto its surface. The lowest I_D/I_G ratio value was for 10%Cr-DLC, which showed the least, from the three samples investigated in this study, population of cell attachment to its surface after conducting the cell seeding procedures. It is apparent that increased Cr content into the growing DLC films alters the microstructure of the deposited films. Furthermore, the density of nano-sized Cr-carbide particles produced during film growth is expected to be the highest in 10%Cr-DLC and the least in 1%Cr-DLC sample. This difference in the Cr-carbide content in the three films is sure to influence the surface chemistry of the DLC films. It was difficult to correlate the water contact angle results with the cell seeding efficiency of the films.

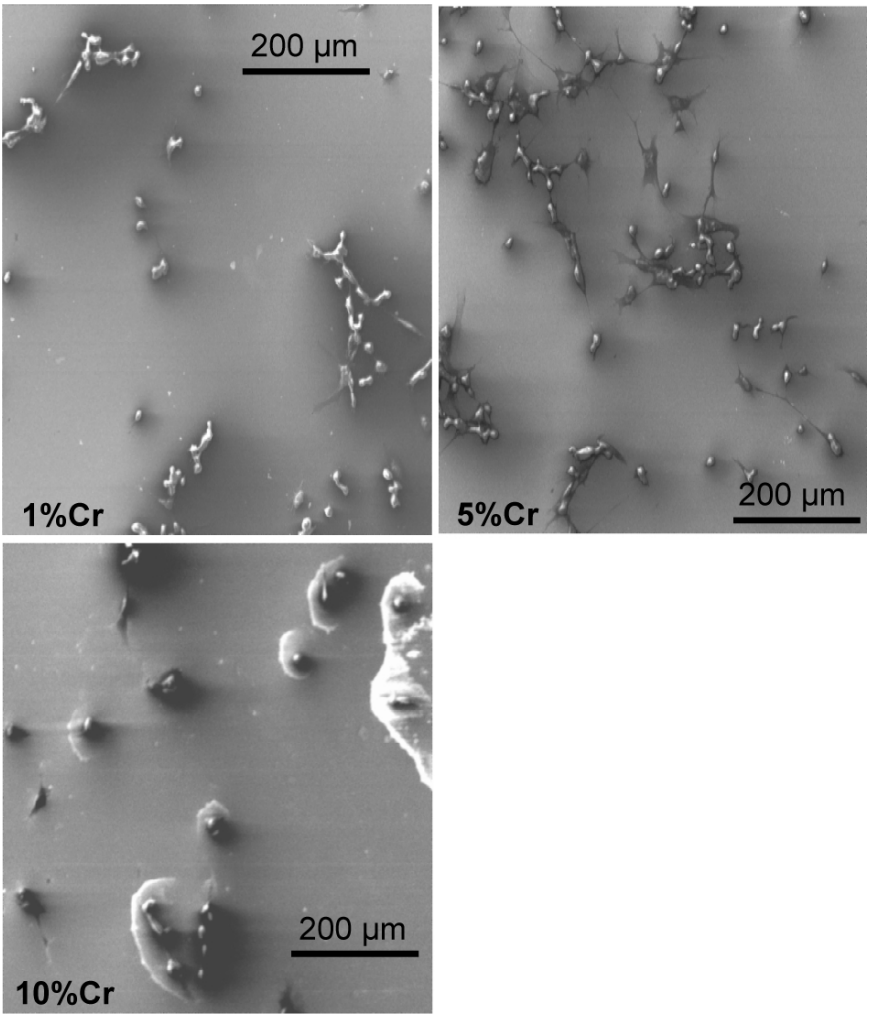

Fig. 6.7. SEM micrographs showing endothelial cell seeding on the three types of Cr-DLC film surfaces

However, Grinell [95] reported that wettable (hydrophilic) surfaces tend to be more conducive to cell adhesion than similar hydrophobic surfaces.

6.6.4 Silicon Modified DLC

We investigate to evaluate the potential of a more readily available synthetic silicon modified carbon film (Si-DLC) for thrombo-resistant

applications. We study the adhesion and spreading of micro-vascular endothelial cells on the surface of Si-DLC and thermally annealed Si-DLC films. Table 6.4 shows the deposition conditions employed for preparing DLC and Si-DLC film samples.

Raman spectroscopy was used to characterise both the as deposited and the thermally annealed DLC and Si-DLC films. The thermal annealing was conducted at temperatures between 200℃ and 600℃ under a flowing nitrogen atmosphere for 2 hours. The information collected from the Raman spectroscopy investigation included the Raman-peak intensities for the D and G-peaks, that is I_D and I_G peaks, the I_D/I_G ratios and the full-width at half maximum (FWHM) for both peaks as shown in Table 6.5.

Table 6.4. deposition conditions for the DLC and Si-DLC film (The numbers in SD5, SD10, SD15 and SD20 represents the flow rates of TMS in sccm used during deposition)

Sample	**DLC**	**SD5**	**SD10**	**SD15**	**SD20**
DC-Volts (volts)	400	400	400	400	400
RF-power (watts)	~150	~160	~165	~175	~210
Temperature (^{o}C)	ambient	ambient	ambient	ambient	ambient
Pressure (base)/torr	6×10^{-6}	6×10^{-6}	6×10^{-6}	6×10^{-6}	6×10^{-6}
Gas ratio (sccm) Ar : C_2H_2: TMS	10:20: 0	10:20:5	10:20:10	10:20:15	10:20:20
Pressure (deposition)/mtorr	$\sim 1.3 \times 10^{-2}$	$\sim 1.9 \times 10^{-2}$	$\sim 2.7 \times 10^{-2}$	$\sim 3.2 \times 10^{-2}$	$\sim 4.5 \times 10^{-2}$
Time (deposition)/mins	5	5	5	5	5

Table 6.5. Raman features of a-C:H and a-C:H:Si thin films

Bias Volts (V)	**TMS sccm**	**I_D (a.u)**	**I_G (a.u)**	**FWHM (D)**	**FWHM (G)**	**I_D/I_G**	**D-Peak (cm^{-1})**	**G-Peak (cm^{-1})**
400	5	1231.7	4397.6	211	104.6	0.28	1336.48	1504.99
400	10	1383.2	6396.5	192.8	103.5	0.21	1310.1	1490.07
400	15	2206.7	9687.6	198.8	103.4	0.22	1296.36	1483.18
400	20	1584.4	8423.5	205.5	102.7	0.18	1278.99	1477.16
400	0	1775.9	4501.8	194.8	108.5	0.39	1349.5	1541.96

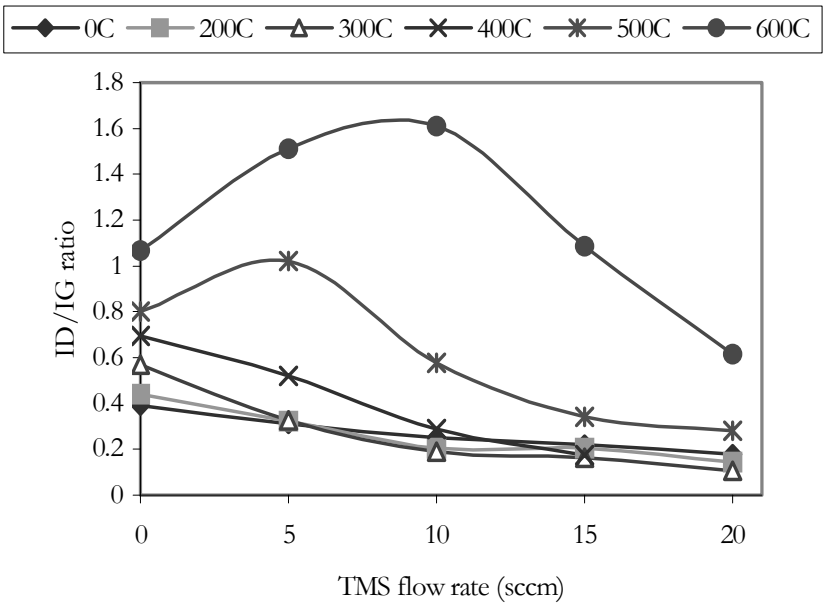

Fig. 6.8. Raman I_D/I_G ratios for the DLC and Si-DLC films both non-annealed and thermally annealed (200-600°C) under flowing nitrogen for 2 hours versus the TMS flow rate during deposition

The results of the Raman spectroscopy show an increase in the I_D/I_G ratios (Fig.6.8) with annealing temperature for the DLC and Si-DLC films in agreement with earlier reports in the literature [96]. The increase in I_D/I_G ratio on the annealing of DLC has been associated with the growth of crystallite structures in the DLC thin film. In the DLC films the increase in the I_D/I_G ratio with thermal annealing is linear, but for the Si-DLC films the I_D / I_G ratio increase occurred only at relatively higher annealing temperatures of 300°C and above. The I_D/I_G ratio also decreases with increasing amount of silicon in the films as shown in Fig.6.8.

Physical and chemical changes in carbon materials resulting in graphitisation occurs during thermal annealing. Graphitisation is associated with an increased sp^2 content, while silicon doping tends to increase the number of sp^3 sites [96]. Silicon does not form π-bonds and it therefore increases the number of sp^3 sites in the Si-DLC films.

Typical x-ray photoelectron spectroscopy (XPS) chemical analysis for the as deposited and annealed DLC and Si-DLC films are as indicated in Table 6.6. The peak binding energies of the films are

Table 6.6. XPS chemical analysis and binding energies (B.E) of elements in the as-deposited DLC and Si-DLC thin films

Sample	C(%)	Peak B.E/eV	O(%)	Peak B.E/eV	Si(%)	Peak B.E/eV
DLC/undoped/400V	89.58	285.11	10.07	532.51	0.36	102.41
DLC(SD5)/400V	82.83	285.01	12.21	533.31	4.96	101.51
DLC(SD10)/400V	79.07	285.09	13.32	533.09	7.61	101.29
DLC(SD15)/400V	76.57	285.10	13.80	533.10	9.63	101.30
DLC(SD20)/400V	77.09	285.10	12.29	533.10	10.62	101.30

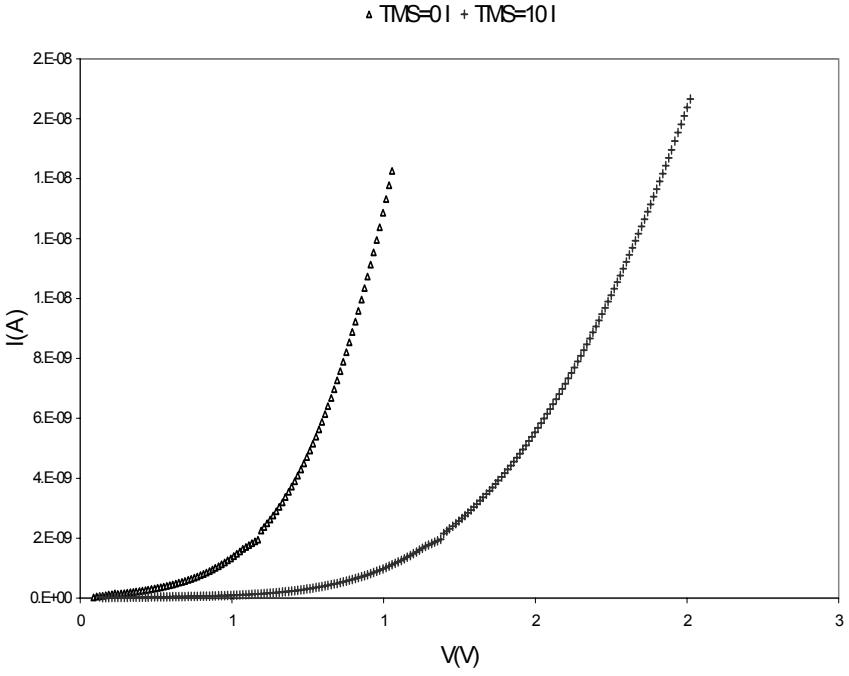

Fig. 6.9. Typical current-voltage (I-V) curves of DLC and Si-DLC (TMS flow rate of 10sccm)

consistent with those reported in the literature by Dementjev [97], Grill [98], Constant and Le Normand [99] and Baker and Hammer [100]. There was only a slight change in the values of the binding energies for the silicon-modified films even after annealing to 600°C. We also observed an increase in sp^3/sp^2 ratios after peak de-convolution.

Typical I-V curves of the metal-semiconductor-metal (MSM) sandwich (Fig. 6.9) shows that the electrical conduction mechanism is not simple ohmic but semi-conducting. We observed that silicon addition to DLC lowers it's resistivity. Thermal annealing of both DLC and Si-DLC leads to a decrease in resistivity (Fig. 6.10), which is likely to be associated with microstructural changes as indicated by the sp^3/sp^2 ratio changes observed for the annealed films by Raman spectroscopy.

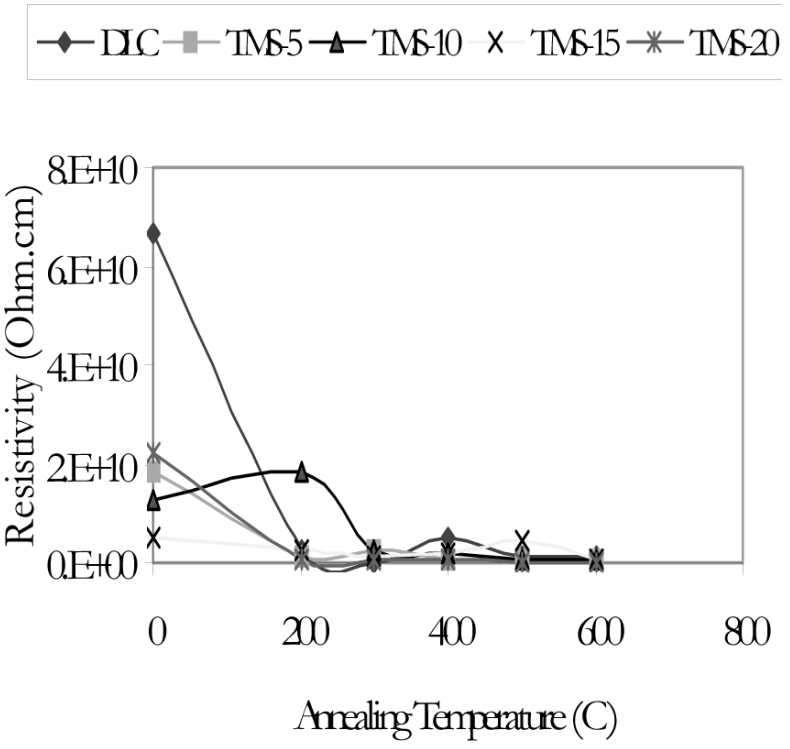

Fig. 6.10. Resistivity versus annealing temperature of DLC and Si-DLC films thermally annealed at 200°C-600°C (on x-axis 0 indicates room temperature)

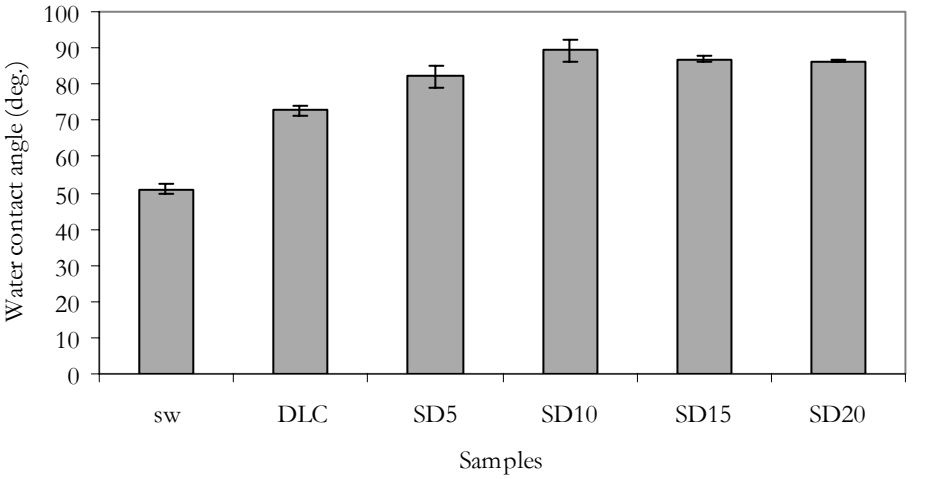

Fig. 6.11. Contact angle in water using direct optical technique

When thermal annealing at 600°C, the conductivity of both DLC and Si-DLC becomes simple Ohmic. This result is consistent with the Raman spectroscopy investigation, which revealed graphitisation at this annealing temperature. The increasing graphitic content of the films at an annealing temperature of 600°C increases the proportion of de-localised π-bonded electrons and therefore increases the electrical conductivity of the films at this annealing temperature, which results in the ohmic-behaviour.

The contact angle measurement results obtained using the optical method are as shown in Fig. 6.11 and the results of the surface energy measured by the Wilhemy plate technique for films deposited on silicon substrates are as shown in Table 6.6. Silicon doping leads to an increase in the contact angles as shown in Fig. 6.11. Silicon doping also results in a slight reduction of the surface energy values as shown in Table 6.7.

As shown in Fig. 6.12a, there seems to be a little cell adhesion on the non-doped DLC seeded with endothelial cells in comparison to the silicon modified DLC films Fig. 6.12b. The measured contact angle for the non-doped DLC film is 72° (which is lower than those of Si-DLC, Fig. 6.11). The general trend observed in our experiments based on scanning electron microscopy (SEM) and cell counting

Table 6.7. Surface energy and contact angle measurements for the films deposited on silicon substrates (γ_P = polar components, γ_D = dispersive components, and γ_S = total surface energy)

TMS/sccm	Bias volt (V)	θ_{adv} water (deg.)	θ_{rec} water (deg.)	γ_P mN/m	γ_D nM/m	γ_S mN/m
(DLC)	400	88.01	55.32	1.17	41.05	42.22
(SD5)	400	82.12	49.27	2.5	41.53	44.03
(SD10)	400	89.54	27.7	1.5	35.73	37.24
(SD15)	400	90.76	41.48	1.24	35.88	37.13

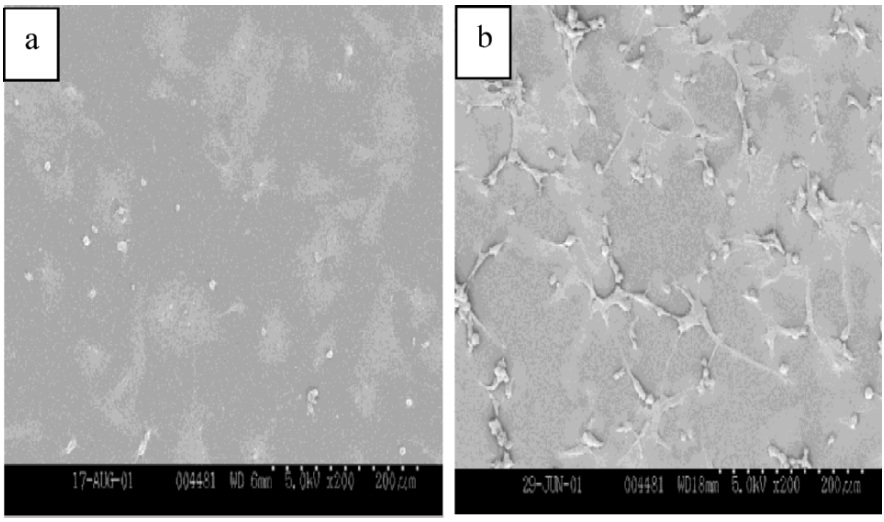

Fig. 6.12. (a) SEM image of DLC seeded with endothelial cells for ~6 hours; x200: (b) Si-DLC (TMS flow rate of 5sccm) seeded with endothelial cells for ~6 hours; x200

using SEM images indicated an increase in cell adhesion with silicon addition in the Si-DLC films. Contrary to earlier reports in the literature by Grinell [101] that wettable (hydrophilic) surfaces tend to be more conducive to cell adhesion, we have observed that more hydrophobic surfaces containing increasing amounts of silicon in the Si-DLC films and increasing contact angle with water, tends to promote human endothelial cell growth and adhesion on the films. The results of the measurements of the surface energy of the DLC and Si-DLC films indicates a substantial contribution to the total surface energy

by the dispersive component term, which might play a part in the cell adhesion process.

The contact potential difference (CPD) measures the surface potential difference between the surface of the films and the vibrating reference electrode made of brass (Cu-Zn). The relationship between the work function of the films $\Phi_{(film)}$, the work function of the reference electrode $\Phi_{(brass)}$ and the CPD is given by:

$$CPD = \Phi_{probe\ (brass)} - \Phi_{sample} = \Phi_{probe\ (brass)} - [\chi + (E_C - E_F)_{bulk}] - \Phi_{ss} \ldots \quad (6.1)$$

The changes in the CPD are related to changes in the electron affinity, χ, band bending due to surface states Φ_{ss}, or a shift of the bulk Fermi level $(Ec\text{-}E_f)_b$. If χ remains constant, then the changes in the CPD are directly related to the shift of the Fermi level in the bulk material and band bending in the surface states [102-104].

The result of the work-function measurements is as shown in Fig. 6.13. The work function decreased with silicon addition. The decrease in work function values has also been associated with a reduction in the net surface dipole [105]. Bolz and Schaldach [106] have already

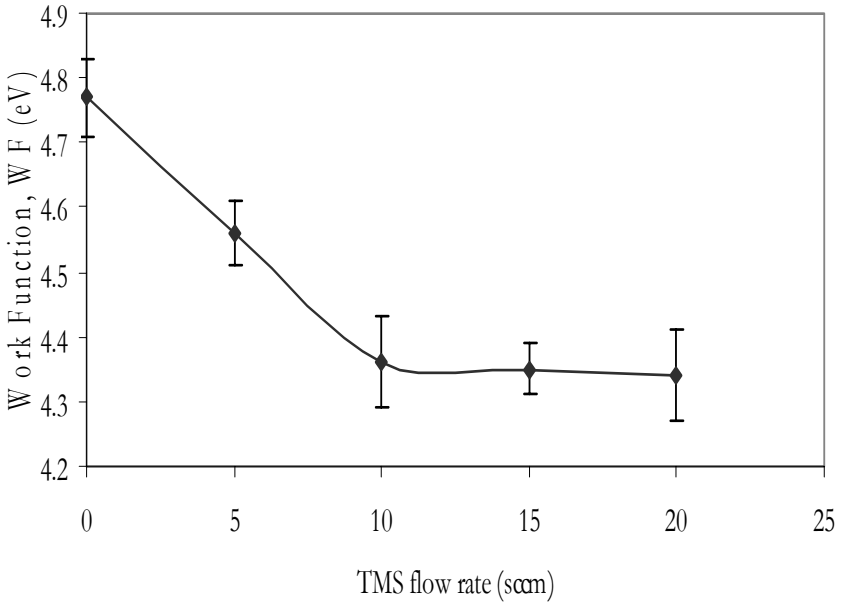

Fig. 6.13. Work function results of DLC and Si-DLC

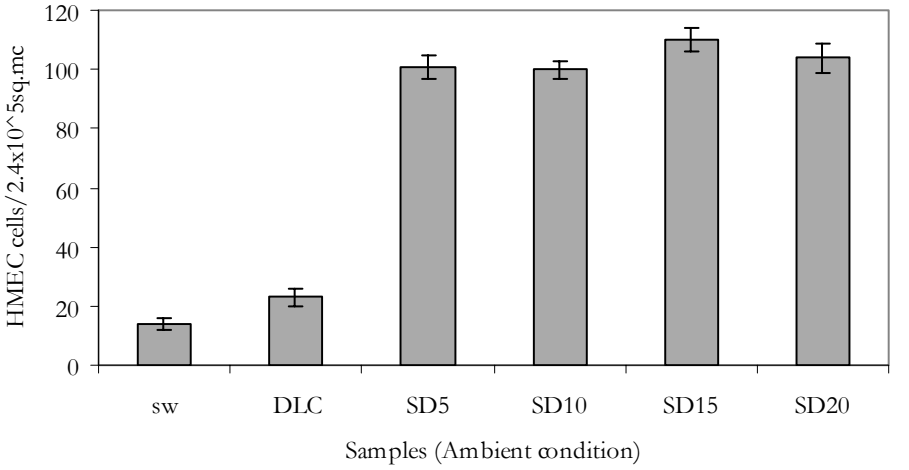

Fig. 6.14. Human micro-vascular endothelial cells (HMEC-1) adhesion on DLC and Si-DLC as obtained (ambient condition, un-annealed samples)

proposed that the early stages of thrombus formation is preceded by an electron transfer oxidation process, resulting in the transformation of fibrinogen to a fibrin polymer. We observed a substantial increase in the number of adherent endothelial cells in the Si-DLC compared to the DLC films as shown in Fig. 6.14, but further silicon addition did not lead to any substantial change in the number of adherent cells on the Si-DLC film surface. It has been suggested that the cell adhesion process depends on the sign of the charge carried by the adherent cell. Positively charged surfaces will attract cells with a negative charge or dipole and vice-versa [106].

The results of the cell count analysis, giving an indication of the adherent cell population against the annealing temperatures are as shown in Figs. 6.15a-c. There is a considerable drop in the population of adherent human endothelial cells for DLC thermally annealed at 600°C compared to the film annealed at 200°C as shown in Fig. 6.15a.The Raman spectrum of the film annealed at 600°C indicates a substantial graphitisation, and this is also the case for the film annealed at 500°C. Annealing DLC at 500°C and 600°C leads to a substantial graphitisation and our current observation is that this does not appear favourable for human endothelial cell adhesion and growth, although the graphite phase is associated with an improvement in electrical

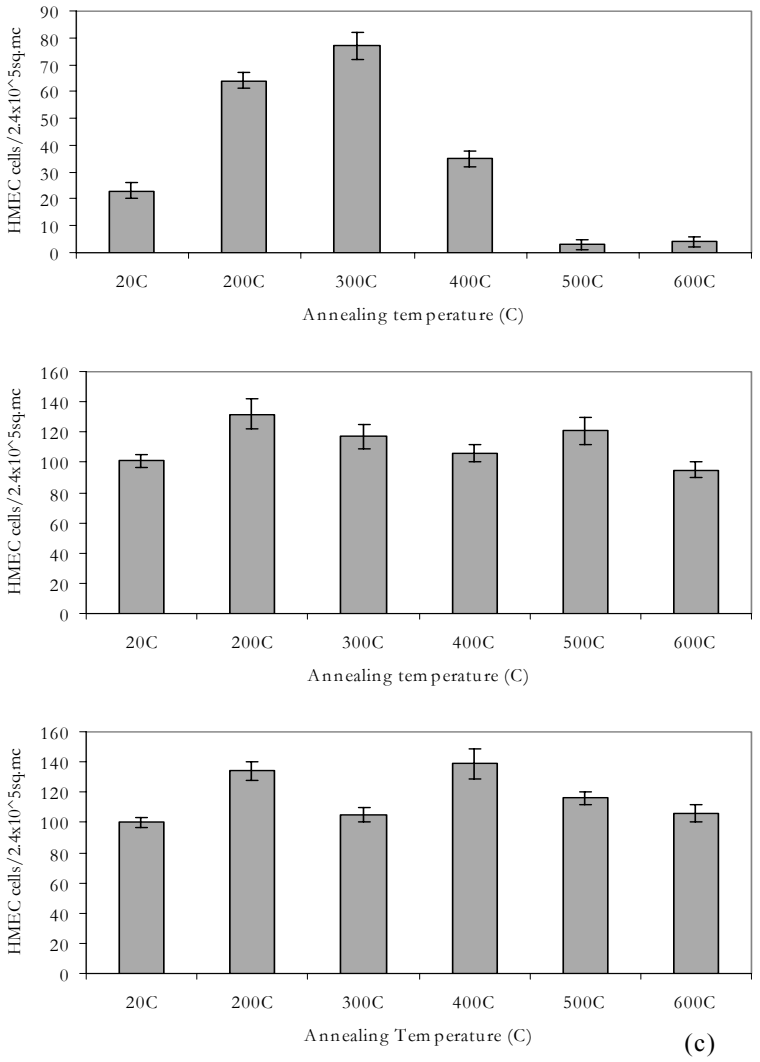

Fig. 6.15. (a) Human endothelial cell adhesion on DLC (as deposited and thermally annealed, 200°C-600°C; 20C = ambient temperature): (b) Si-DLC (TMS flow rate, 5sccm, as deposited and thermally annealed, 200°C-600°C, 20C = ambient temperature); (c) Si-DLC (TMS flow rate, 10sccm, as deposited and thermally annealed, 200°C-600°C, 20C = ambient temperature)

conduction. For the Si-DLC samples annealed between 200°C and 600°C, there was a fairly consistent population of endothelial cells for the 5 and 10sccm TMS flow rate films as shown in Fig. 6.15b

and 6.15c. In all the cases investigated for the DLC and Si-DLC films, we observed a direct correlation between electronic conduction in the films and the population of adherent human endothelial cells whenever there was no significant graphitisation detectable by Raman spectroscopy. However, even when electronic conduction was relatively high in the films, graphitisation in such films always led to a substantial reduction in the population of adherent endothelial cells on it's surface. There is a significant statistical difference in endothelial cell count (at 95% confidence interval level, with $p<0.05$, paired t-test and Tukey test) between the samples DLC and Si-DLC at ambient temperature.

The results of the MTT-assay shown in the histogram in Fig. 6.16, give the optical density of the active cells in culture after fifty-six (56) hours. The averaged-blanks values were subtracted from the total reading in order to take into account the optical density contribution due to the colour of the as-deposited DLC and Si-DLC thin films. This was confirmed by using the reader to read the optical density of the empty culture dishes, both coated and non-coated, and it was observed that there were some readings. The assay detects metabolism in the living cells and the intensity obtained is dependent on the degree of activity of the cells [107]. Further details of the statistical analysis of the MTT assay of HMECs on DLC and Si-DLC films

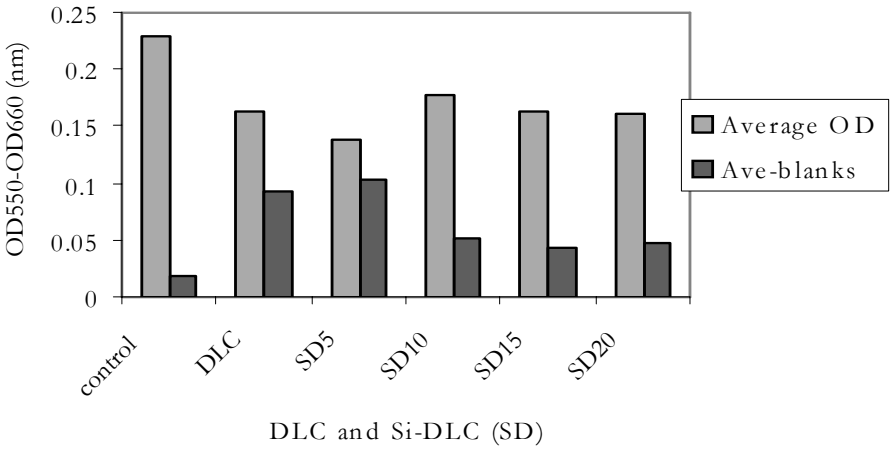

Fig. 6.16. Histogram of MTT-assay of HMEC seeded on 96 well culture plates that were coated with DLC and Si-DLC (TMS flow-rate, 5-20sccm, SD5-20)

using the ANOVA test has been reported elsewhere by some of the authors of this chapter [108].

6.7 Summary

The contents of the current chapter can be summarised as follows:

- Mechanical heart valves were introduced and the principal concerns relating to such valves were put forward.
- The history of mechanical heart valves has been reviewed dating back from 1952.
- The process of thrombosis has been defined, described and the principals of thrombus formation have been outlined.
- The chapter also discusses the hemocompatibility of biomaterials. Further, we describe the endothelium, its functions and endothelial cell seeding in modern biomaterials engineering.
- The hemocompatibility of DLC films has been reviewed and in particular results of investigations on Cr-DLC and Si-DLC films have been presented and discussed.
- The diamond-like films were deposited containing different levels of Cr and Si contents.
- The contact angle measurements showed that the surface contact angle gradually increased with %Cr content in the films films and began to level off at around 10%Cr content.
- Raman spectroscopy was used to characterise the D and G bands present in all the Cr-DLC films.
- The I_D/I_G ratios were correlated to the population of endothelial cell attachments onto Cr-DLC surfaces. High values of I_D/I_G ratio correlate with better HMC-EC attachment to 5%Cr-DLC film. This finding suggests that disordered graphitic phases in the DLC film leads to enhancement in the seeding of endothelial cells.
- With silicon modified DLC films, we observed a direct correlation between adherent cell population on the film surfaces and electronic conduction.

- This correlation does not hold when graphitisation, which is detected by Raman spectroscopy has occurred in the Si-DLC films regardless of their electronic conductivity.
- The micro-structural variation in the films was achieved by varying silicon content and by thermal annealing.
- A direct relationship between increasing contact angle of water (i.e., hydrophobicity) and adherent endothelial cell population was observed. This trend is the opposite of those reported in the literature for other cells, where a hydrophilic interaction was considered necessary for cell attachment on surfaces.
- We suspect that the interaction between endothelial cells and the Si-DLC films could be mediated by dispersive forces.
- Although the work function decreased with increasing silicon addition, and silicon addition lead to an initial increase in the population of adherent endothelial cells on the film surface, further silicon addition did not lead to any substantial changes in the number of adherent endothelial cells on the Si-DLC film surface.
- The cytotoxicity of the endothelial cells on the Si-DLC film was measured by the MTT-assay test and the cells are established to be viable after adhesion to the Si-DLC films.
- The biological response of human microvascular endothelial cells seeded on chromium and silicon modified diamond-like carbon films and on control surfaces was evaluated in terms of initial cell enhancement, growth and cytotoxicity.
- Endothelial cell adhesion and growth was found to be affected by changes in the microstructure of the films induced by chromium/silicon doping and thermal annealing of silicon modified diamond-like carbon films.
- We observed a significant statistical difference in endothelial cell count between DLC and Si-DLC films using the paired t-test.
- MTT-assay tests showed the endothelial cells to be viable when seeded on Si-DLC films before and after thermal treatment based on the ANOVA statistical test.

References

1. K. Barton, A. Campbell, J.A. Chinn, C.D. Griffin, D.H. Anderson, K. Klein, M.A. Moore and C. Zapanta, *Biomedical Engineering Society (BMES) Bulletin*, Vol. 25, No. 1, (2001) 3.
2. C.A. Hufnagel and W.P. Harvey, *Bull. Georgetown Univ. Med. Cent*., 6: 60-63 1953).
3. L. Vincent, M.D. Gott, E. Diane Alejo, and E. Duke, M.D. Cameron, *Ann Thorac Surg* 2003; 76: S2230-S2239.
4. G. Murray, *Angiology*, 7: 466 (1956).
5. N.S. Braunwald, T. Cooper and A.G. Morow, *J. Thorac. Cardiovasc. Surg*., 40: 1-11 (1960).
6. H.T. Bahnson, F.C. Spencer, E.F.G. Busse and F.W. Davis, Jr., *Ann. Surg*., 152: 494 (1960).
7. B.B. Roe, J.W. Owsley and P.C. Boudoures, *J. Thorac. Cardiovasc. Surg*., 36: 563-570 (1958).
8. B.B. Roe, *J. Thorac. Cardiovasc. Surg*., 58: 59-61 (1969).
9. N.S. Braunwald and A.G. Morrow, *J. Thorac. Cardiovasc. Surg*., 49: 485-496 (1965).
10. A. Richard, M.D. DeWall, M.D. Naureen Qasim and Liz Carr, *Ann Thorac Surg* 2000; 69: 1612-21.
11. V.L. Gott, R.L. Daggett, J.D. Whiffen et al., *J. Thorac. Cardiovasc. Surg*., 48: 713-725 (1964).
12. A.B. Cruz, R.L. Kaster, R.L. Simmons, C.W. Lillehei, *Surgery* 1965; 58: 995-8.
13. J. Wada, S. Lomatsu, K. Ikeda et al., A new hingeless valve. In: *Prosthetic Heart Valves* (Brewer, L.A., editor), Springfield Thomas, pp. 304-314 (1969).
14. V.O. Björk, *J. Thorac. Cardiovasc. Surg*., 3: 1-10 (1969).
15. R. Carmen and S.C. Mutha*, J. Biomed. Mater. Res*., 6: 327-346 (1972).
16. V.O. Björk, *The Surgical Treatment of Aortic Valve Disease*. Ingelhelm and Rhein, C.H. Boehringer Sohn, (1974).
17. B.J. Messmer, M. Rothlin and A. Senning, *J. Thorac. Cardiovasc. Surg*., 65, 386-390 (1973).
18. V.L. Gott, J.D. Whiffen and S.M. Valiathan, *Ann. NY. Acad. Sci.,* 146: 21-29 (1968).
19. S.M. Scott, G.K. Sethi, A.H. Bridgman and T. Takaro, *Ann. Thorac. Surg*., 21: 483-486 (1976).
20. A.C. Beall, Jr., G.C. Morris, Jr., G.P. Noon et al., *Ann. Thorac. Surg*., 15: 25-34 (1973).
21. Cedars-Sinai Medical center Prosthetic heart valve information, Division of Cardiology: http://www.csmc.edu/pdf/Heart_Valves.pdf
22. C.W. Lillehei, R.L. Kaster, M. Coleman and J.H. Bloch, NY *State Med. J*.,74: 1426-1438 (1974).
23. FDA panel meeting for approval of the OmniCarbon®valve,PMA# P830039, 1998.
24. di Summa, M. Poletti, Breno, L. et al*., J Heart valve Dis* 2002; 11: 517-23.

25. P.J.K. Starek, L.P. McLaurin, B.R. Wilcox, G.F. Murry, *Ann. Thorac. Surg*., 22: 362-368 (1976).
26. P.J.K. Starek, R.L. Beaudet and V.K. Hall, The Medtronic-Hall valve: Development and clinical expe-rience. In: *Cardiac Surgery Current Heart Valve Prosthesis* (Crawford, F.A., ed.), Hanley & Belfus,Philadelphia, pp. 223-236,1987.
27. *Food and Drug Administration Enforcement Report*, September 7, (1988).
28. W.P. Young, R.L. Daggett, VL. Gott, Long-term follow-up of patients with a hinged leaflet prosthetic heart valve. In: Brewer L.A., ed. *Prosthetic heart valves*. Springfield, IL: Charles C. Thomas, (1969) 622-32.
29. B.R. Kalke, *Evaluation of a double-leaflet prosthetic heart valve of a new design for clinical use*, Ph.D. Thesis, University of Minnesota, (1973).
30. *Lessons of Björk-Shiley Heart Valve Failure*. www.me.utexas.edu/~uer/ heartvalves/shiley.html.
31. J.J. Klawitter, Design and in vitro testing of the Duromedics bileaflet valve. *First International Hemex Symposium on the Duromedics Bileaflet Valves* (1985).
32. R. Richard, A. Beavan and P. Strzepa*, J. Heart Valve Dis*., 3: S94-S101 (1994).
33. J. Craver, Carbomedics Prosthetic Heart Valve(tm). *Euro Jl Cardio-Thorac. Surg*. 15 (Suppl.1) S3-Sll (1999).
34. Prosthetic heart valves: History of mechanical heart valve replacement: *BMES BULLETIN*; No4: vol. 24, (2000).
35. A. Campbell, T. Baldwin, G. Peterson, J. Bryant and K. Ryder, *J. Heart Valve Dis.*, 5: S124-S132 (1996).
36. B. Lung, T. Haghigat, E. Garbaz et al., Incidence and predictors of prosthetic thrombosis on mitralbileaflet prostheses during the postoperative period. *Congress of the European Society of Cardiology*, August 1999.
37. E. Bodnar, P. Arru, E.G. Butchard et al., Panel discussion, *J. Heart Valve Dis*., 5: S148 (1996).
38. J. Gross, M. Shu, F. Dai, J. Ellis and A. Yoganathan, *J. Heart Valve Dis*., 5: 581-590 (1996).
39. http://www.accessdata.fda.gov/scripts/cdrh/cfdocs/cfTopic/mda/mda-cardio.cfm?topic=421>
40. M.H. Henri Spronk, Danielle van der Voort and Hugo ten Cate, *Thrombosis Journal* 2004, 2: 12 doi: 10.1186/1477-9560-2-12.
41. William DF (ed.) *Definitions in Biomaterials*, Elsevier, (1987)b.
42. S.H. Teoh, *International Journal of Fatigue* 22 (2000) 825-837.
43. A. Klinger D. Steinberg, D. Kohavi & M.N. Sela, (1997), *J. Biomed. Mater. Res*. 36: 387-392.
44. BMEn 5001-"cardiovascular" *Applications of Biomaterials*; November 25, 1998-W.Gleason.
45. http://www.biomed.metu.edu.tr/courses/term_papers/artif-heart-valves_erol.htm
46. C.E. Soltys-Robitaille, D.M. Ammon, Jr. , P.L. Valint Jr. and G.L. robe III, *Biomaterials* 2001; 22: 3257-3260.

47. V. Pesakova, Z. Klezl, K. Balik, M. Adam. *Journal of Material Science: Materials in Medicine* 2000; 11(12): 793-798.
48. G.M. Bruinsma, H.C. Van der Mei, H.J. Busscher. *Biomaterials* 2001: 22; 3217-3224.
49. A. Ahluwalia, G. Basta, F. Chiellini, D. Ricci, G. Vozzi, *Journal of Material Science: Materials in Medicine* 2001; 12(7): 613-619.
50. G.L. Bowlin and S.E. Rittger. *Cell Transplantation* 1997; 6(6): 623-629.
51. P.B. Van Wachem, J.M. Schakenraad, J. Feijen, T. Beugeling, W.G. Van Aken, E.H. Blauuw, P. Nieuwenhius, I. Molenaar. *Biomaterials* 1989; 10: 532-539.
52. S.D. Bruck, *Polymer* 1975; 16: 25.
53. S.D. Bruck, *Nature* 1973; 243: 416-417.
54. S.D. Bruck, *J. Poly Sc* 1967; C17: 169-185.
55. A. Boldz, M. Schaldach, *Artificial Organs* 1990; 14(4): 260-269.
56. J.Y. Chen, L.P. Wang, K.Y. Fu, N. Huang, Y. Leng, Y.X. Leng, P. Yang, J. Wang, G.J. Wan, H. Sun, X.B. Tian, P.K. Chu, *Surface and Coatings Technology* 2002; 156: 289-294.
57. http://greenfield.fortunecity.com/rattler/46/endothelium.htm
58. http://teaching.anhb.uwa.edu.au/mb140/MoreAbout/Endothel.htm
59. J.L. Gordon, 1986 in *Blood-Surface Interactions: Biological Principles Underlying Hemocompatibility with Artificial Materials* edited by Cazenave J.P, Davies J.A, Kazatchkine M.D, and W.G van Aken; Elsevier Science Publishers (Biomedical Division) 1986; pp. 5.
60. S. Williams, *Cell Transplantation* 4: 401-410, 1994.
61. T. Horbett, *Colloids Surf. B: Biointerfaces* 2: 225-240, 1994.
62. Veli-Matti Tianen, *Diamond and Related Materials* 10 (2001) 153-160.
63. A. Grill, B.S. Meyerson, Development and status of diamondlike carbon, in K.E. Spear, J.P Dismukes (eds), *Synthetic Diamond; emerging CVD science and technology*, Wiley, New York, 1994, Chapter 5.
64. A. Schroeder, G. Francz, A. Bruinink, R. Hauert, J. Mayer, E. Wintermantel, *Biomaterials* 21 (5) (2000) 449-456.
65. R. Hauert, L. Knoblauch-Meyer, G. Francz, A. Schroeder, E. Wintermantel, *Surf. Coat. Technol.* 120-121 (1999) 291-296.
66. R. Hauert, U. Muller, G. Francz, et al., *Thin Solid Films* 308-309 (1997) 191-194.
67. A. Dorner-Reisel, C. Schurer, C. Nischan, O. Seidel, E. Muller, *Thin Solid Films* 420-421 (2002) 263-268.
68. R. Hauert, U. Muller, *Diamond and Related Materials* 12 (2003) 171-177.
69. N. Huang, P. Yang, Y.X. Leng, J. Wang, J.Y. Chen, H. Sun, G.J. Wan, A.S. Zhao and P.D. Ding, "Surface Modification for Controlling the Blood-Materials Interface": invited report on *6th Asia Symposium on Biomedical Materials*, July 20-23, 2004, Chengdu, China and published in *Key Engineering Materials* http://www.paper.edu.cn/scholar/download.jsp?file=huangnan-6
70. Y.X. Leng, N. Huang et al., *Surface Science*, Vol. 531 (2003), p. 177.

71. P. Yang, J.Y. Chen, Y.X. Leng, H. Sun, N. Huang, P.K. Chu, 7th International Workshop on Plasma Based Ion Implantation, Sept. 16-20, 2003, San Antonio, USA, 2003.
72. N. Huang, P. Yang, Y.X. Leng, J. Wang, H. Sun, J.Y. Chen, G.J. Wan, *Surface & Coatings Technology* 186 (2004) 218- 226.
73. P. Yang, S.C.H. Kwok, P.K. Chu, Y.X. Leng, J.Y. Chen, J. Wang, N. Huang, *Nuclear Instruments and Methods in Physics Research*. Section B, Beam Interact. Mater. Atoms 206 (2003) 721.
74. M.I. Jones, I.R. McColl, D.M. Grant, K.G. Parker, T.L. Parker, *Diamond and and Related Materials* 8 (1999) 457-462.
75. M.I. Jones, I.R. McColl, D.M. Grant, K.G. Parker, T.L. Parker, *J. Biomed. Mater. Res.* 52/2 (2000) 413-421.
76. I. Dion, X. Roques, C. Baquey, E. Baudet, B. Basse Cathalinat, N. More, *Bio-Med. Mater. Eng*. 3y1 (1993) 51-55.
77. F.Z. Cui and D.J. Li., *Surf. Coat. Technol*. 131 (2000), pp. 481-487.
78. K. Gutensohn, C. Beythien, J. Bau, T. Fenner, P. Grewe, R. Koester, K. Padmanaban and P. Kuehnl, *Thrombosis Research* 99 (2000) 577-585.
79. A. Alanazi, C. Nojiri, T. Noguchi, T. Kido, Y. Komatsu, K. Kirakuri, et al., *ASAIO* J. 46 (2000) 440-443.
80. L.A. Thomson, F.C. Law, N. Rushton, J. Franks, *Biomaterials* 12 (1991) 37.
81. M. Allen, F. Law, N. Rushton, *Clin. Mater*. 17 (1994) 1.
82. I. De Scheerder, M. Szilard, H. Yanming, et al., *J. Invasive Cardiol*. 12 (8) (2000) 389-394.
83. A. Schroeder, G. Francz, A. Bruinink, R. Hauert, J. Mayer, E. Wintermantel, *Biomaterials* 21 (5) (2000) 449-456.
84. G. Francz, A. Schroeder, R. Hauert, *Surf. Interface Anal*. 28 (1999) 3.
85. R. Hauert, L. Knoblauch-Meyer, G. Francz, A. Schroeder, E. Wintermantel, *Surf. Coat. Technol.* 120-121 (1999) 291-296.
86. R. Hauert, U. Muller, G. Francz, et al., *Thin Solid Films* 308-309 (1997) 191-194.
87. A. Schroeder*, Ph.D. Thesis*, Dissertation Nr. 13079, ETH Zurich (1999).
88. A. Dorner-Reisel, C. Schurer, C. Nischan, O. Seidel, E. Muller, *Thin Solid Films* 420-421 (2002) 263-268.
89. P. Yang, N. Huang, Y.X. Leng, J.Y. Chen, H. Sun, J. Wang, F. Chen and P.K. Chu, *Surface and Coatings Technology*, 156 (2002) 284-288.
90. J.Y. Chen, Y.X. Leng, X.B. Tian, L.P. Wang, N. Huang, P.K. Chu and P. Yang, *Biomaterials*, 23 (2002) 2545-2552.
91. Y.X. Leng, H. Sun, P. Yang, J.Y. Chen, J. Wang, G.J. Wan, N. Huang, X.B. Tian, L.P. Wang and P.K. Chu, *Thin Solid Films*, 398-399, (2001) 471-475.
92. Y.X. Leng, P. Yang, J.Y. Chen, H. Sun, J. Wang, G.J. Wang, N. Huang, X.B. Tian and P.K. Chu, *Surface and Coatings Technology*, 138 (2001) 296-300.
93. J. Li, *Biomaterials*, 14 (1993) 229.
94. A.A. Adjaottor, E. Ma and E.I. Meletis, *Surface and Coatings Technology,* 89 (1997) (3), pp. 197-203.

95. F. Grinnell, *Int. Rev. Cytol*. 1978; 53: 65-144.
96. A.A. Ogwu, R.W. Lamberton, S. Morley, P. Maguire, J. McLaughlin. *Physica B* 1999; 269: 335-344.
97. A.P. Dementjev, M.N. Petukhov, A.M. Baranov, *Diamond and Related Materials* 1998; 7: 1534-1538.
98. A. Grill, B. Meyerson, V. Patel, J.A. Reimer and M.A. Petrich, *J. Applied Physics*, 1987; 6: 2874.
99. L. Constant, Le Normand, *Diamond and Related Materials* 1997; 6: 664-7.
100. M.A. Baker and P. Hammer, *Surface and Interface Analysis* 1997; 25: 629-642.
101. F. Grinnell, *Int. Rev. Cytol*. 1978; 53: 65-144.
102. D.P. Magill, A.A. Ogwu, J.A.D. McLaughlin, P.D. Maguire, *J. Vac. Sci. Technol. A* 2001; 19(5): 2456-2462.
103. A. Hadjaj, R.E. Cabarrocas, B. Equar, *Philosophical Magazine* 1997; B76:941.
104. A. Hadjaj, M. Favre, B. Equer, R.I. Cabaroccas, *Solar Energy Materials and Solar Cells* 1998; 51: 145-153.
105. G. Attard and C. Barnes, *Surfaces* 1998; Oxford University Press: 64-65.
106. A. Boldz, M. Schaldach, *Artificial Organs*, 1990; 14(4): 260-269.
107. H. Wan, R.L. Williams, P.J. Doherty, D.F. Williams, *Journal of Materials Science: Materials in Medicine* 1994; 5: 441-445.
108. T.I.T. Okpalugo, E. McKenna, A.C. Magee, J.A. McLaughlin, N.M.D. Brown, *Journal of Biomedical Materials Research Part A*, 2004; 71A (2): 201-208.